AIP | Physics of Plasmas
#1 JOURNAL IN 2014 GOOGLE SCHOLAR METRICS FOR THE PLASMA & FUSION CATEGORY

Ion acceleration by intense, few-cycle laser pulses with nanodroplets

Laura Di Lucchio, Alexander A. Andreev, and Paul Gibbon

Citation: Physics of Plasmas **22**, 053114 (2015); doi: 10.1063/1.4921667
View online: http://dx.doi.org/10.1063/1.4921667
View Table of Contents: http://scitation.aip.org/content/aip/journal/pop/22/5?ver=pdfcov
Published by the AIP Publishing

Articles you may be interested in

On the analysis of inhomogeneous magnetic field spectrometer for laser-driven ion acceleration
Rev. Sci. Instrum. **86**, 033303 (2015); 10.1063/1.4914845

Multi-charged heavy ion acceleration from the ultra-intense short pulse laser system interacting with the metal targeta)
Rev. Sci. Instrum. **85**, 02B904 (2014); 10.1063/1.4827111

Conditions for efficient and stable ion acceleration by moderate circularly polarized laser pulses at intensities of 1020 W/cm2
Phys. Plasmas **18**, 043102 (2011); 10.1063/1.3577573

Thin tape target driver for laser ion accelerator
Rev. Sci. Instrum. **74**, 3293 (2003); 10.1063/1.1578156

Intense ion beams accelerated by ultra-intense laser pulses
AIP Conf. Proc. **611**, 199 (2002); 10.1063/1.1470305

VACUUM SOLUTIONS FROM A SINGLE SOURCE

Pfeiffer Vacuum stands for innovative and custom vacuum solutions worldwide, technological perfection, competent advice and reliable service.

125 YEARS NOTHING IS BETTER

This article is copyrighted as indicated in the article. Reuse of AIP content is subject to the terms at: http://scitation.aip.org/termsconditions. Downloaded to IP: 134.94.122.242 On: Tue, 18 Aug 2015 12:55:05

Ion acceleration by intense, few-cycle laser pulses with nanodroplets

Laura Di Lucchio,[1] Alexander A. Andreev,[2] and Paul Gibbon[1,3]
[1]*Forschungszentrum Jülich GmbH, Institute for Advanced Simulation, Jülich Supercomputing Centre D-52425 Jülich, Germany*
[2]*Max Born Institute, Max Born Str. 2a, D-12489 Berlin, Germany*
[3]*Centre for Mathematical Plasma Astrophysics, Department of Mathematics, KU Leuven, Celestijnenlaan 200B, 3001 Heverlee, Belgium*

(Received 27 March 2015; accepted 12 May 2015; published online 27 May 2015)

The energy distribution of electrons and ions emerging from the interaction of a few-cycle Gaussian laser pulse with spherical nanoclusters is investigated with the aim of determining prospects for accelerating ions in this regime. It is found that the direct conversion of laser energy into dense attosecond electron nanobunches results in rapid charge separation and early onset of Coulomb-explosion-dominated ion dynamics. The ion core of the cluster starts to expand soon after the laser has crossed the droplet, the fastest ions attaining 10 s of MeV at relativistic intensities. The current investigation should serve as a guide for contemporary experiments, i.e., using state-of-the-art few-cycle ultraintense lasers and nanoclusters of solid density. © *2015 AIP Publishing LLC*. [http://dx.doi.org/10.1063/1.4921667]

I. INTRODUCTION

Ion acceleration by short-pulse, high-intensity lasers has been actively pursued for the last 15 years following the landmark experiments detecting MeV protons from gold foils with PW-class laser systems at the turn of the millennium.[1–3] Since then, despite enormous progress in laser technology and targetry, the maximum ion energies achieved have remained stubbornly below expectations: proton energies up to 50 MeV (Ref. 4) and to more than 60 MeV have been recently recorded[5] with laser systems on paper capable of producing proton beams with many 100 s of MeV. One problem with these sources has been their generally broad (Maxwellian-like) energy spectrum, which is not favorable for many potential applications demanding a quasi-monoenergetic beam with 1% bandwidth or better.[6] These limitations have spawned a host of schemes for improving the energy and quality of ion beams such as: mass-limited targets,[7] radiation pressure acceleration,[8] light-sail,[9] and Break-Out-Afterburner (BOA).[10]

Of these numerous regimes of ion acceleration, a number involve laser-cluster interaction, the idea being that mass-limited targets are more conducive to creating high degrees of charge separation and so result in larger accelerating fields. Early work with rare gas clusters had the purpose of finding suitable conditions for hydrodynamical expansion or Coulomb explosion of multicharged clusters irradiated by intense lasers ($10^{15}\,\mathrm{W/cm^2} < I < 10^{20}\,\mathrm{W/cm^2}$).[11,12] Deuterium molecular clusters were typically used to determine experimental conditions for complete outer ionization and electron expulsion,[13] with a corresponding maximum attainable ion energy of a few hundreds of keV. The proton energy spectrum from laser-irradiated hydrogen clusters in an intermediate regime between hydrodynamical expansion and Coulomb expansion has been studied in Ref. 14. In Ref. 15, the regime of Coulomb explosion for hydrogen droplets has been studied in more detail, finding more intermediate energy spectra shapes for ions.

A general threshold intensity for expelling all the electrons can be found which predicts maximum proton energies of the order of MeV and above. Such energies represent the necessary step for making the laser-cluster configuration competitive with other ion acceleration mechanisms. In Refs. 16 and 17, fast ion spectra for laser-illuminated micron-sized spheres are compared to equivalently irradiated targets with different geometry. It is found that when the dimension of the target does not exceed the laser focus size, rounded targets can enhance the energy of the accelerated ions. Experimental work carried out recently at MBI in Berlin, where water droplets of 20 μm diameter were illuminated by short laser pulses of 35 fs duration and $I = 10^{19}\,\mathrm{W/cm^2}$, obtained backward and forward emission and maximum ion energies up to 1.5 MeV (Refs. 18 and 19).

Extending these previous works, we investigate whether two-cycle ultraintense pulses are also able to extract high-energy ions from submicron solid-density clusters and we compare our results with the results from longer pulse interactions similar to those so far used in experiments. The remainder of this paper will be structured as follows: First, a summary of the previous results for electron acceleration in this regime will be given, in order to describe the general physical context in which the ion dynamics starts to take hold. Then, the applicability of known models of the three main regimes of ion acceleration will be explored and evaluated by means of varying the droplet size and the laser intensity. These are, respectively, Coulomb explosion, isothermal expansion—equivalent to Target Normal Sheath Acceleration (TNSA), and finally, the more challenging intermediate regime. Further discussion on the possibility of shock generation for small droplets and relatively high intensity precedes final conclusions.

II. ELECTRON DYNAMICS

We have performed 2D simulations with EPOCH particle-in-cell code,[20] using a sphere of pre-ionized hydrogen plasma with 100 n_c density containing 34×10^6 particles, placed at the center of a 20 μm × 20 μm box with open

 © 2015 AIP Publishing LLC

This article is copyrighted as indicated in the article. Reuse of AIP content is subject to the terms at: http://scitation.aip.org/termsconditions. Downloaded to IP: 134.94.122.242 On: Tue, 18 Aug 2015 12:55:05

boundaries. The simulations have been run sufficiently long to determine the characteristic time for the ion cloud expansion, which is typically 200 fs after the start of the interaction.

We have considered clusters whose radius is much smaller than the laser focus, namely, 100–200 nm, and compared their dynamics with a cluster of 1 μm radius, that is, of the same size of the focus. For the latter, a ten times higher resolution statistics has been used, so that the number of particles was 340×10^6, and the box was enlarged up to 40 μm $\times$ 40 μm. The laser is modeled as a tightly focused linearly polarized 2-cycle Gaussian pulse, with a duration of 5 fs; the focus size was chosen to be 1 μm, while the laser wavelength was 800 nm. The intensity of the laser was varied between 5×10^{18} and 10^{21} W/cm^2, in order to infer scaling laws for the emitted particles' energies and to identify any transitions in the cluster ion dynamics.

The electrons are expelled from the nanodroplet during the first 10 fs after the onset of the interaction with the laser, and their dynamics depends on both the droplet size and the laser intensity (see Refs. 21 and 22). Such a dependence is in contrast to what has been previously obtained in the study of low-density helium droplets irradiated by 16-cycle laser pulses by Liseykina *et al.*,[23] where Mie theory determines the directional emission of the electrons independently of the laser intensity. For droplets whose size is much smaller than the laser focus, namely, with a radius ranging from 100 to 500 nm, overcritical dense electron plasma regions which can be identified as isolated nanobunches are emitted every half-cycle, following two symmetric directions with respect to the x axis (whereas the laser is polarized along y axis) in good agreement with ponderomotive scattering model predictions.[24] Immediately after emission, these bunches travel together with the transmitted portion of the laser pulse, which for the smaller droplets constitutes most of the wave energy, since reflection and diffraction are minimal. This is evident from the plots of the transmitted energy density (Fig. 1), which when superimposed on the electron number density show the spatial coincidence of electron nanobunches and field null points.

Subsequently, the orientation of the bunches changes in time due to further interaction of the outgoing electrons with the ponderomotive force of the transmitted electromagnetic wave in vacuum. Conversely, the laser field itself is perturbed by the current formed by the emitted electrons. The final detectable emission angle (determined in the near field) turns out to be both size and intensity-dependent, showing a strong deviation from optical Mie theory for relativistic intensities (see Ref. 21). Droplets whose size is comparable to the laser focus, namely of 500 nm radius or bigger, exhibit

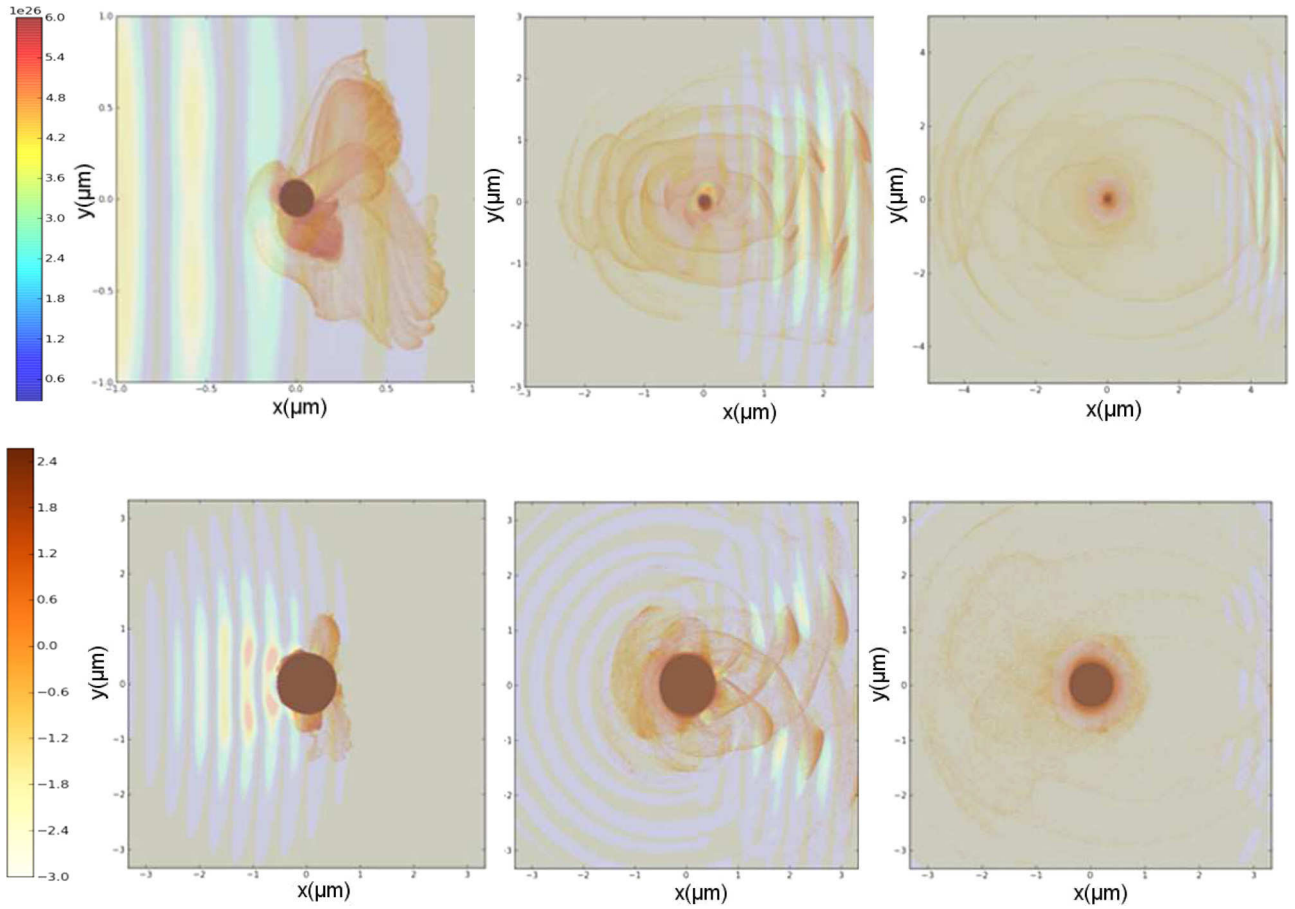

FIG. 1. Energy density and electron number density (superposed) for a 100 nm droplet (up) and a 1 μm droplet (down) in a temporal sequence from left to right, namely: at the beginning of the interaction with the laser pulse moving from left to right (t = 5 fs after the initial hit), during the interaction (t = 15 fs), and after the interaction (t = 25 fs). The jet color scale is valid for energy density, whereas the electron number density is represented by a logarithmic YlOrBr color scale.

This article is copyrighted as indicated in the article. Reuse of AIP content is subject to the terms at: http://scitation.aip.org/termsconditions. Downloaded to IP: 134.94.122.242 On: Tue, 18 Aug 2015 12:55:05

electron dynamics strongly affected by the optical phenomena depicted in Fig. 1. A larger droplet is seen by the laser wave as an opaque obstacle, and therefore, the pulse is both reflected and diffracted; the electron emission pattern is then more complicated, showing the superposition of an intense flux along the directions predicted by Mie theory and of the proper nanobunches production. Both for the small and the big droplet case, Fig. 1 shows how the energy density decreases in the transmitted pulse while this is traveling in the vacuum, and no high energy density peak is observed, in contrast with what happens with reflected pulses from thin foils. This is more evident in the case of the 1 μm droplet, which shows a reflected pulse of appreciable field strength—that is, of the same order as of the transmitted one—at the end of the laser-bunch interaction. More details of these processes can be found in Refs. 21 and 22.

III. ION DYNAMICS

In order to investigate ion dynamics properly, the new and challenging regime exposed by the two-cycle pulse has been compared to the already explored case of a 40 fs pulse. In low-density He droplets, interacting with 40 fs pulses a directional ion emission has been observed, following Mie predictions[23] for the local electric field enhancement on the surface, leading to a dominant electron emission angle. In the cases studied here with solid density droplets, no directional emission of the ions is observed because the electron bunches themselves have negligible influence on the ion motion. The electron bunches are emitted along the directions predicted by the model in Ref. 22 every half cycle of the laser; therefore, the electron dynamics can be considered to be almost of the same kind for a short and long pulse. In both cases, an underdense electron cloud remains behind together with the expanding ions at least for the first 100 fs of interaction. However, the two-cycle laser pulse allows a faster dynamic for the electron bunches, which leave the droplet within 10 fs, thus decoupling the main electron emission mechanism from the ion motion. Also, a 5 fs laser is less efficient in removing the electron cloud. After the bunches have escaped in vacuum, a hot electron cloud is formed around the cold ion core. The ions start to expand in the ambipolar field created by the surrounding negative charge at about t = 50 fs after the interaction with the laser.

The energy spectra of the ions in Fig. 2 exhibit an intermediate shape between thermal and Coulomb explosion, apart from intensities much greater than $10^{20}\,\mathrm{W/cm^2}$. This means that such TNSA ions exhibit peculiar behaviors which are worth investigating in more detail. We therefore review the theoretical treatments available for the two extreme cases of Coulomb explosion vs. thermal expansion before introducing a hybrid model which better describes the intermediate regime. This will allow us to better distinguish the resulting situations in the parameter space of interest.

A. Coulomb explosion

The condition stated by Sakabe *et al.*[15] for expelling all of electrons from the cluster can be here invoked for Coulomb explosion, and reads as

$$a > \left(\frac{8\pi Ze^2 n}{3mc^2}\right)^{1/2} \equiv 34\left(\frac{\mathrm{Zn}}{5\times 10^{22}\,\mathrm{cm^{-3}}}\right)^{1/2}\left(\frac{R}{1\,\mu\mathrm{m}}\right). \quad (1)$$

Using the parameters of interest here, namely, Z = 1 and R = 100 nm, it turns out that the threshold for the value of

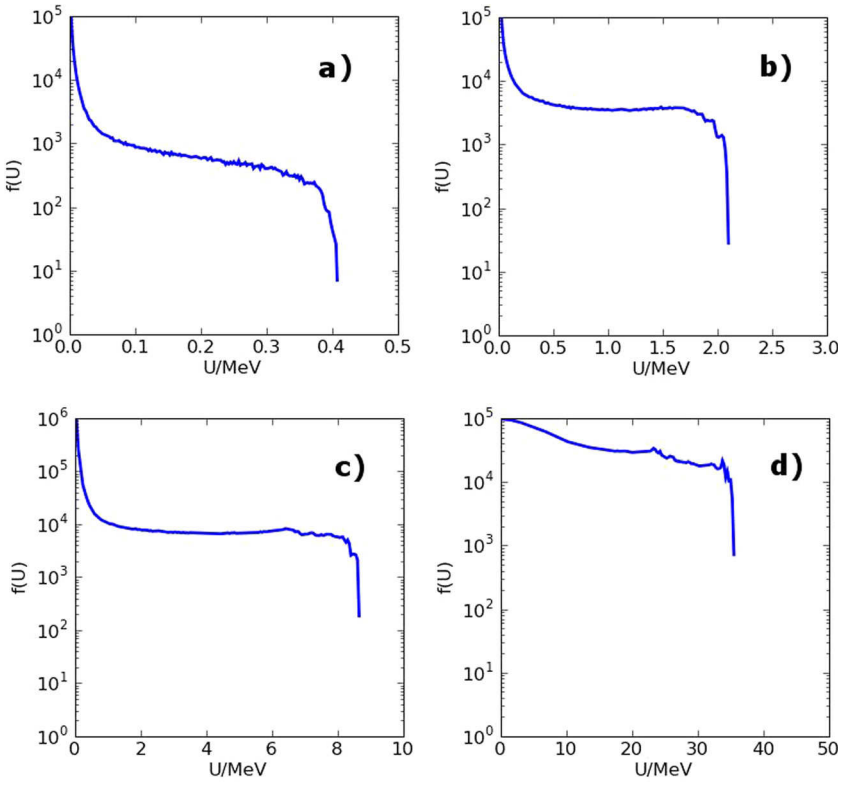

FIG. 2. Energy spectra for ions at t = 200 fs in a 100 nm radius droplet hit by a 5 fs laser pulse of intensity I = $10^{18}\,\mathrm{W/cm^2}$ (a), I = $10^{19}\,\mathrm{W/cm^2}$ (b), I = $10^{20}\,\mathrm{W/cm^2}$ (c), and I = $10^{21}\,\mathrm{W/cm^2}$ (d). Energy in MeV/c^2, momenta in MeV/c.

This article is copyrighted as indicated in the article. Reuse of AIP content is subject to the terms at: http://scitation.aip.org/termsconditions. Downloaded to IP: 134.94.122.242 On: Tue, 18 Aug 2015 12:55:05

dimensionless amplitude $a = eE/m\omega c$ is $a_{th} \approx 6.3$, which means that for $I = 5 \times 10^{20}\,W/cm^2$ the Coulomb regime should be entered. This transition is visible in Fig. 4, where the maximum ion energy in the case of interaction with a 5 fs and a 40 fs pulse, respectively, tends to reach similar values at intensities close to $10^{21}\,W/cm^2$. The slight difference in final energies can be explained by assuming, analogously to the study in Ref. 13, that a sufficiently small hydrogen cluster will be characterized by the explosion time

$$\tau_{Coul} \approx 0.8\sqrt{\frac{4\pi\varepsilon_0 m_p}{n_p e^2}}, \tag{2}$$

where m_p and n_p are the proton mass and number density ($n_p = 1.72 \times 10^{23}\,cm^{-3}$), respectively. This characteristic time is required for the droplet to double its radius R, independently of the value of R itself, and can be used for clusters which cannot be ionized to high charge state, such as hydrogen. Using our parameters, one can estimate $\tau_{Coul} \approx$ 6.5 fs, which means that our two-cycle laser pulse is just below the threshold duration for the expulsion of most of the electrons together with the bunches. In fact, the final ion energy is close, but not equal to the maximum attainable one which is characteristic of the interaction with longer laser pulses.

The ion spectra in Fig. 2 represent instead the intermediate expansion regime that we are most interested in. Previous work on ion acceleration from mass-limited targets by Limpouch *et al.*[16,17] dealt with the interaction of a relativistic laser pulse with large droplets of radius $\approx 4\lambda$, and estimated the average energy of hot electrons accelerated at the target front size as equivalent to the ponderomotive potential, namely

$$\varepsilon_h \approx m_e c^2(\gamma_L - 1), \gamma_L = \sqrt{1 + a_0^2} = \sqrt{1 + 0.7 \times I_{18}\lambda_{L,\mu m}{}^2}. \tag{3}$$

Here, γ_L is the relativistic gamma factor of electron oscillation in the laser field, I_{18} is the laser intensity in units of $10^{18}\,W/cm^2$, and $\lambda_{L,\mu m}$ is the laser wavelength in microns. According to this treatment, the hot electron temperature scales as $\sim I^{1/2}$. Such a dependence is shown for our parameters in Fig. 3, together with the simulation results for different droplet sizes.

B. Isothermal expansion (TNSA)

In Fig. 3, a fit has been calculated over the hot electron energy spectrum considering a number of particles ranging from 10^3 to 10^5, and a set of characteristic temperatures has been found spanning over the laser intensities and droplet sizes. The resulting behavior only approximately follows the $I^{1/2}$ dependence predicted by Eq. (3) over the droplet sizes considered but with a marked inverse correlation with radius.

In the case of pure isothermal expansion, we can define the characteristic acceleration time $t_{ef} \approx t_L$, where t_L is the laser pulse duration. An estimate for the cutoff energy of the ions can be obtained by means of an asymptotic treatment of the self-similar solution to the hydrodynamics equations for the ion fluid[25] in the quasi-neutral isothermal approximation.[17]

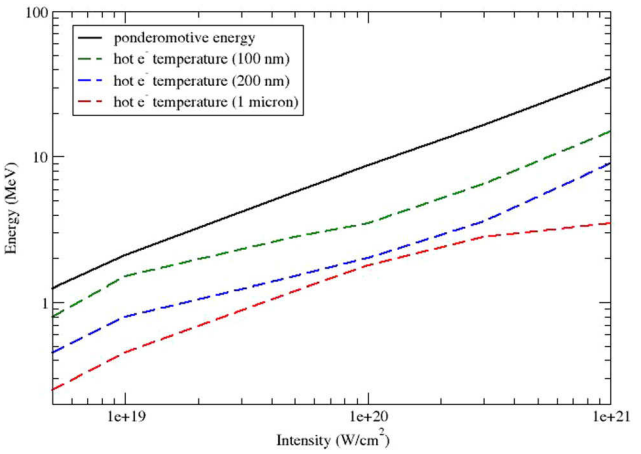

FIG. 3. Dependence on laser intensity of the characteristic temperature in the hot electron cloud surrounding the ion core soon after the bunches' emission, for different droplet sizes, against the ponderomotive energy formula.

In this context, cylindrical geometry is assumed. By integrating the equations of motion of an individual ion in the field obtained by unifying asymptotic calculations at early and later times, one gets for the maximum ion energy the following expression:

$$\varepsilon_{im} \approx Z\varepsilon_{eh}\ln^2\left(c_s t_{ef}/r_{dh} + \sqrt{(c_s t_{ef}/r_{dh})^2 + 1}\right), \tag{4}$$

where $r_{dh} \approx (\varepsilon_h/4\pi e^2 n_{eh}{}^{1/2})$ is the hot electron Debye radius. The results of formula (4) have been compared to the simulation data for both small and bigger droplets in Fig. 4. From the density output, it has been inferred that the density of the electron cloud surrounding the ion core ranges between the critical density and ten times its value.

C. Intermediate regime

In Fig. 4, the maximum ion energies determined from simulations for the 5 fs and 40 fs pulse are presented. In the

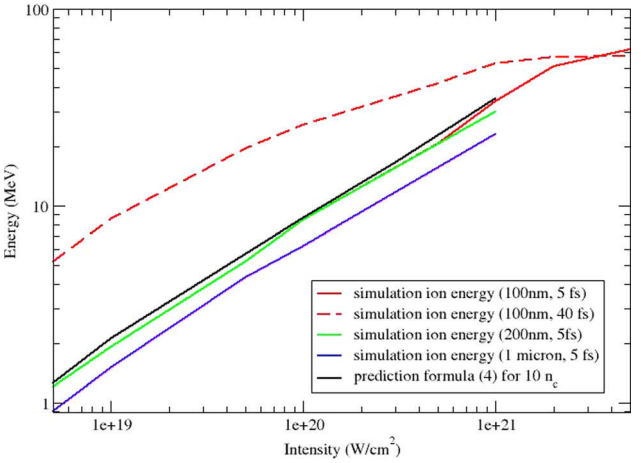

FIG. 4. Dependence of maximum ion energy on laser intensity and on pulse duration, for different droplet sizes, against the hydrodynamical model. For the sake of simplicity, the comparison between maximum attainable ion energy with the 2- and 16-cycle laser pulses is only shown for a 100 nm droplet. In all cases, energy values are measured 200 fs after the start of the laser-cluster interaction.

This article is copyrighted as indicated in the article. Reuse of AIP content is subject to the terms at: http://scitation.aip.org/termsconditions. Downloaded to IP: 134.94.122.242 On: Tue, 18 Aug 2015 12:55:05

case of the longer pulse, the behavior of E_{max} is similar to the $I^{1/2}$ dependence predicted for a rare gas cluster in Ref. 13. By contrast, the 5 fs laser pulse exhibits a growth approximately as $\sim I^{2/3}$ until it reaches the pulse duration independent Coulomb explosion value for laser intensities just above 10^{21} W/cm^2. For pulse intensities between 2×10^{21} W/cm^2 and 5×10^{21} W/cm^2, the simulation points corresponding to the short pulse case start to overcome the corresponding ones related to the long pulse interaction. Therefore, one could infer that at even higher intensity there could be a gain in energy with the two-cycle laser pulse.

A completely analytical model for the hydrodynamical expansion of a spherical cluster has been developed by Murakami and Basko[26] and subsequently used for practical calculations in the context of the interpretation of experiments with laser-illuminated water droplets. Such a treatment has been developed to address the problem of ion acceleration during the self-similar expansion of finite-size non-quasi-neutral plasmas into vacuum, and is based on constructing a self-similar solution for the hydrodynamical equations under the assumption of an asymptotic linear velocity-radius relation. For the complete set of equations and similarity relations, the reader is referred to Ref. 26.

The corresponding physical system of the cluster expansion after the interaction with a laser field has two characteristic scale lengths, namely, the plasma size $R(t)$ and the hot electron Debye length $\lambda_D(t) = \sqrt{T_e/4\pi n_e e^2}$. If $R(t)$ and $\lambda_D(t)$ evolve coherently in time, that is, if the ratio between them is kept constant as a single and invariant dimensionless parameter, namely

$$\Lambda = \frac{R}{\lambda_D} = R_0 \left(\frac{4\pi e^2 n_{e0}}{T_{e0}} \right)^{1/2}, \tag{5}$$

then a self-similar solution for the cluster expansion can be found. Defining $\mu_e = Zm_e/m_i$ as the electron-ion mass-over-charge ratio, for $\Lambda \gg 1$, and $\mu_e \ll 1$, the self-similar solution for the ion front position ξ_f is the same for all geometries (linear, cylindrical, spherical) and reads

$$\xi_f^2 = W(0.5\Lambda^2), \tag{6}$$

where W(x) is the inverse of the function $x = We^{xp}(W)$, also called as the Lambert W function. Asymptotically, $W(x) \approx x$ for $x \ll 1$ and $W(x) \approx \ln(x/\ln x)$ for $x \gg 1$.

The maximum ion energy is then determined by the following formula:

$$\xi_{i,\max} = \varepsilon_{i0} \xi_f^2, \tag{7}$$

where the bulk ion energy ε_{i0} in the spherical case can be expressed as

$$\varepsilon_{i0} = 2ZT_{e0}. \tag{8}$$

Finally, the ion distribution function is in the following form:

$$\frac{dN_i}{d\varepsilon} \approx \frac{N_{i0}}{\varepsilon_{i0}} \sqrt{\frac{\varepsilon}{\varepsilon_{i0}}} \left[\frac{1}{\Lambda^2} + \exp\left(-\frac{\varepsilon}{\varepsilon_{i0}} \right) \right], \tag{9}$$

TABLE I. Analytical value of Λ as it can be inferred by formula (7) after evaluating Lambert function with standard numerical approximation, for a 100 nm droplet hit by a laser at different intensities. The corresponding maximum energy of the ions is of the order of MeV, showing a nearly stationary behavior.

I (W/cm^2)	E_0 (MeV)	Λ	ξ_f^2	$E_{i,\max}$ (MeV)
5×10^{18}	1.6	3.49	1.44	2.3
1×10^{19}	3.0	1.44	0.5	1.74
5×10^{19}	5.6	1.05	0.38	2.12
1×10^{20}	7.0	0.94	0.32	2.24
3×10^{20}	13.0	0.69	0.19	2.47

where N_{i0} is the total number of cluster heavy ions. For $\Lambda < 1$, there is a pure Coulomb explosion case. For our parameters, $\Lambda \approx 1$; therefore, we have an intermediate case between thermal expansion and Coulomb explosion. For a big parameter Λ, the function (10) has a local maximum at $\varepsilon_{imax} \approx ZT_{e0}$.

In practical cases with spherical geometry, a suitable estimate for the validity of the limit (7) is $\Lambda \gg 50$. In cylindrical geometry, the restriction is $\Lambda \gg 5$. In our case, however, simulations indicate that the temperature averaged over the electron cloud is of the order of a few MeV, which means that one must expect $\Lambda \approx 1$. For example, taking $K_B T_{e0} = 0.8$ MeV, $n_{e0} = 1.72 \times 10^{22}$ cm^{-3} (or 10 n_c) and $R_0 = 100$ nm $= 10^{-5}$ cm, a straightforward calculation in cgs units yields ($e = 4.8 \times 10^{10}$ statC, 1 MeV $= 1.6 \times 10^{-6}$ erg) $\Lambda = 3.49$. Correspondingly, one has $W(0.5\Lambda^2) = 1.44$ and $E_{i,\max} = 2.3$ MeV, which is fairly within the expected order of magnitude (see Fig. 4). However, further calculations show how the Lambert function approximation (7) fails in determining the maximum ion energy dependence on the laser intensity (see Table I).

The results in Table I can be explained in a straightforward way, if one better analyzes the hydrodynamical equations in Ref. 26. The analytical treatment allows one to find a solution in terms of known mathematical function in the following cases: $\Lambda \gg 1$, $\mu_e \ll 1$ (all geometries), $\Lambda \ll \mu_e^{1/2}$ (linear and planar geometries), $\Lambda \ll \mu_e^{3/4}$ (spherical

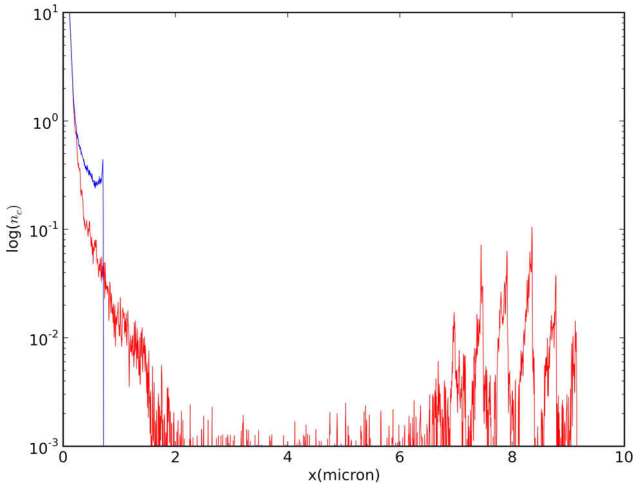

FIG. 5. Electron and ion logarithmic density plots for a 100 nm droplet hit by a $I = 10^{20}$ W/cm^2 laser pulse at t = 70 fs after the start of the interaction.

This article is copyrighted as indicated in the article. Reuse of AIP content is subject to the terms at: http://scitation.aip.org/termsconditions. Downloaded to IP: 134.94.122.242 On: Tue, 18 Aug 2015 12:55:05

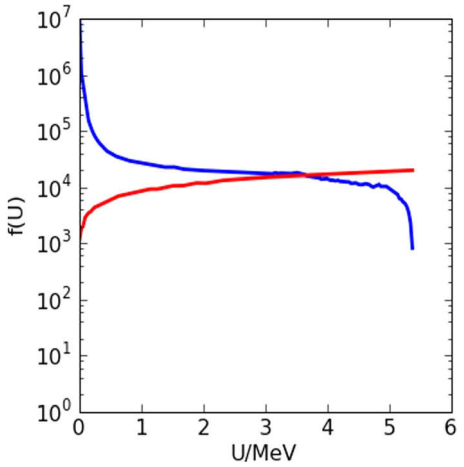

FIG. 6. Phase plots and energy spectrum (top right) for a 100 nm droplet struck by a $I = 10^{20}$ W/cm^2 laser pulse, at $t = 70$ fs after the laser interaction. The energy spectrum (blue) is superposed to the curve corresponding to the formula (10), calculated using the actual energies of the single particles in the simulation.

geometry). For the intermediate case when $\Lambda \approx 1$, no analytical solution exists.

In Fig. 5, the electron and ion densities are plotted at the time $t = 70$ fs after the start of the interaction. The bunches are clearly visible, and the ion and electron densities take on forms qualitatively similar to those described by the Murakami and Basko model. However, the energy spectrum is not well described by formula (10), as one can see in Fig. 6. After this time, the expansion causes a complete superposition of the ion and electron densities, thus changing the physical picture with respect to this model.

In Fig. 7, we can observe the electron and ion temperatures at such time.

IV. DISCUSSION: MULTIDIMENSIONAL EFFECTS AND SHOCK FORMATION

In order to get a more detailed picture of the subsequent expansion, the ion and electron densities have been analyzed separately making use of both 2D graphs and 1D profiles (see Figs. 8–11). In particular, the intermediate case between thermal and Coulomb expansion is shown, regarding, respectively, a 100 nm (Figs. 8 and 9) and a 1 μm (Figs. 10 and 11) droplet hit by a laser pulse of intensity $I = 10^{20}$ W/cm^2, first for the short and then for the long pulse. A two-cycle laser pulse appears to be able to leave in the ion cloud an imprint of early surface plasma waves, which can be still seen 60 fs after the beginning of the interaction. Such periodic density perturbations have been thoroughly investigated for a pure ionized hydrogen droplet in Ref. 27 for nonrelativistic intensities. In our simulations, instead, they appear to be washed out soon after the initial phase of the expansion; their early existence is shown in the 2D density plots in Figs. 8 and 10.

For a 16-cycle laser pulse, such waves are naturally levelled out by the action of the electromagnetic field crossing the expanding cloud, whereas the ion expansion begins while the latest electron bunches are still being extracted by the laser (see Figs. 9 and 11). For the smallest droplets (up to 500 nm radius), the expansion is accompanied by the formation of a shock located at the outer shell, as in Fig. 10. The shock acceleration is responsible for the highest proton energies, while the TNSA ions show a nearly isotropic emission, as observed in Ref. 7. This is peculiar of spherical mass-limited targets, which exhibits a very different behavior from planar shaped ones. The generation of ion-accelerating shocks in slabs has been thoroughly investigated in Ref. 28; the behavior of shock shell formation in nanoclusters has been previously examined in Ref. 29. In Ref. 7, a more detailed numerical analysis is performed, but it is limited to micron-sized spheres whose diameter is bigger than the laser focus and whose density is only a few times the critical one (although the simulations are compared with experiments using analogous targets with solid density). Following this treatment, we can extend the general formula for the velocity of a shock propagating outside a target irradiated by a high-intensity laser to our problem. The formula was used already in earlier work by Wilks *et al.*[30] to describe hole-boring in ultraintense laser-plasma interactions

$$\frac{v}{c} = \frac{a_L}{\sqrt{2}} \left(\frac{m_e}{m_i}\right)^{1/2} \left(\frac{n_c}{n_i}\right)^{1/2}, \tag{10}$$

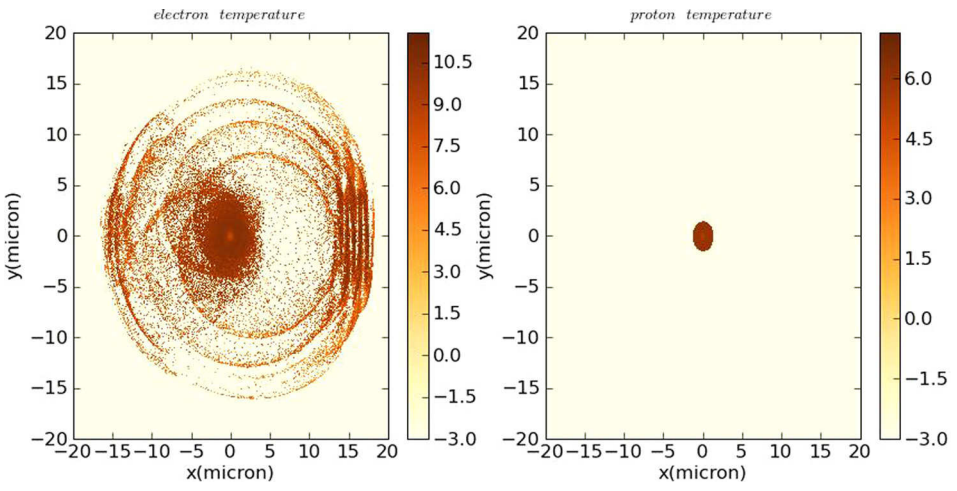

FIG. 7. Logarithm of ion and electron temperatures in Kelvin for a 100 nm droplet irradiated by a $I = 10^{20}$ W/cm^2 laser pulse, at $t = 70$ fs after interaction with the laser.

This article is copyrighted as indicated in the article. Reuse of AIP content is subject to the terms at: http://scitation.aip.org/termsconditions. Downloaded to IP: 134.94.122.242 On: Tue, 18 Aug 2015 12:55:05

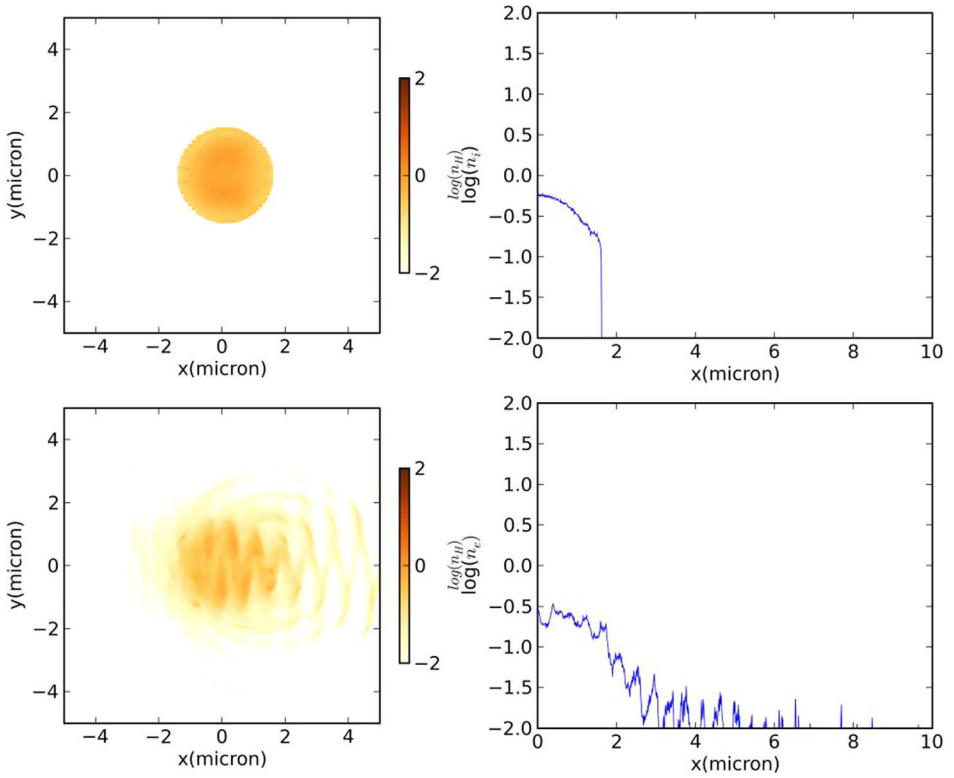

FIG. 8. Ion (above) and electron (below) density at t = 60 fs after the initial laser-droplet interaction, for a 100 nm radius droplet hit by a laser pulse of 40 fs duration and intensity I = 10^{20} W/cm^2. The density scale is logarithmic and goes up to 100 n_c.

where $a_L = a_0 f(r)$ is the radius-dependent laser amplitude for our Gaussian pulse. Taking $a_L \equiv a_0 = 6.83$ ($I = 10^{20}$ W/cm^2), we get $v = 0.35c$, which is a remarkable velocity for the shock shell, enough to accelerate ions to MeV energies as with planar mass-limited targets. The ion cloud crosses the open boundaries of the 20 μm box at about 250 fs after the start of the interaction, and the radial density profile clearly shows the motion of the shock shell towards these boundaries (see Fig. 10, right side). Similar to what happens in Ref. 29, the size of the sphere plays a role in the shock formation and propagation: in clusters whose radius is close to the laser focus extension shock acceleration is no more the

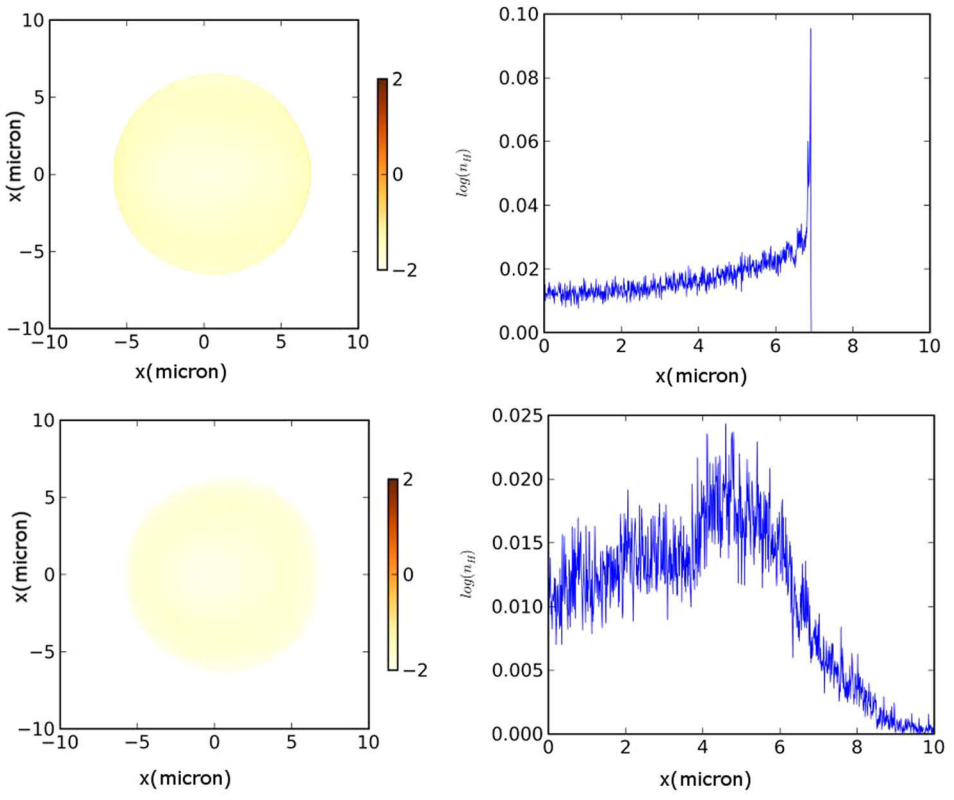

FIG. 9. Ion (above) and electron (below) density at t = 150 fs after the initial laser-droplet interaction, for a 100 nm radius droplet hit by a laser pulse of 40 fs duration intensity I = 10^{20} W/cm^2. The density scale is logarithmic and goes up to 100 n_c.

This article is copyrighted as indicated in the article. Reuse of AIP content is subject to the terms at: http://scitation.aip.org/termsconditions. Downloaded to IP: 134.94.122.242 On: Tue, 18 Aug 2015 12:55:05

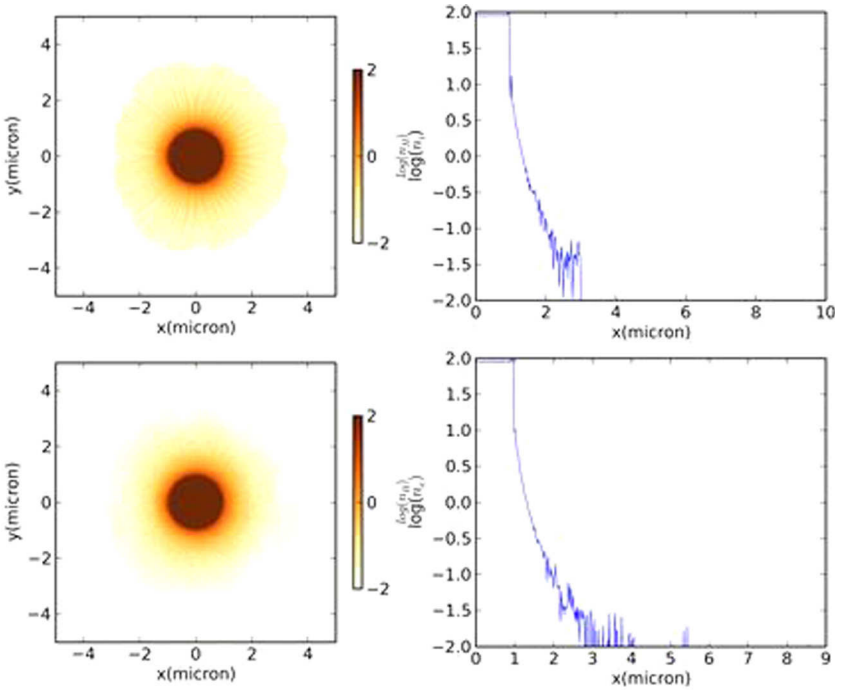

FIG. 10. Ion (above) and electron (below) density at t=100 fs after the initial laser-droplet interaction, for a 1 μm radius droplet hit by a laser pulse of 5 fs duration and intensity I = 10^{20} W/cm^2. The density scale is logarithmic and goes up to 100 n_c.

prevalent mechanism for the ion of gaining energy, and only the hydrodynamic expansion is responsible for that both at early and later times (see Fig. 11).

V. CONCLUSIONS

We have investigated the existence of scaling laws for the maximum energies of both electron and ion clouds emitted quasi-isotropically by ultraintense laser irradiated droplets of different sizes. Furthermore, we have compared our results in the case of a two-cycle and a 16-cycle laser pulse, and we have shown that the gain in the final ion energy is not proportional to the pulse length; instead, the two-cycle pulse leads to a stronger scaling of the ion energies with laser intensity, saturating at the point when the electrons are completely stripped from the cluster. Finally, we have fitted our simulation data making use of the already existing models for depicting the transition from thermal expansion at the lowest laser intensities, up to Coulomb explosion at the highest. It is found that, for the smallest droplets ($R \approx 100 - 500$ nm), the highest energies can be obtained both in the case of a two-cycle and of a 16-cycle laser pulse. Both cases are interesting, because the maximum ion energies achievable with a 2-cycle pulse shows a dependence $\sim I^{2/3}$, which corresponds to a steeper ascent than in the long pulse

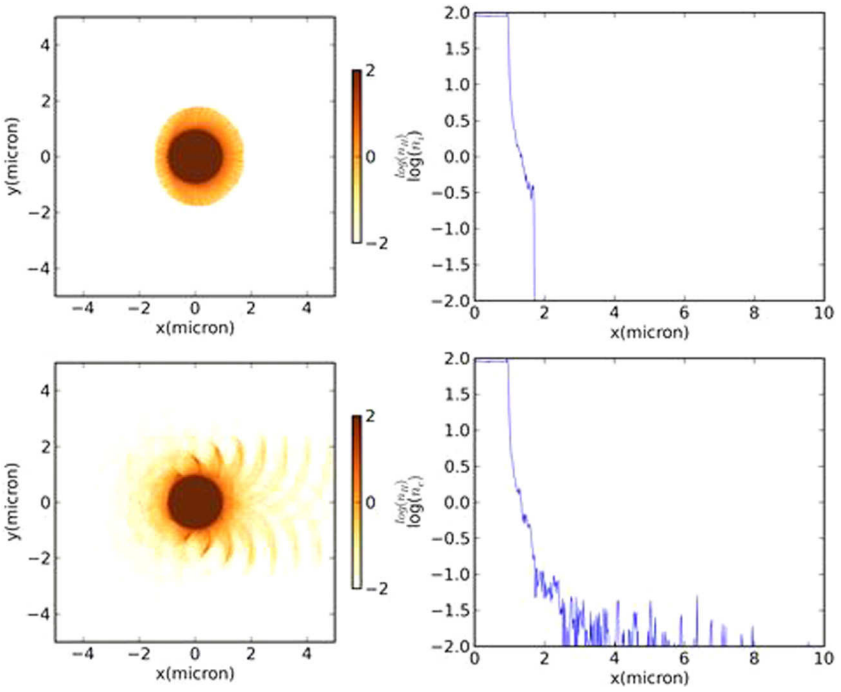

FIG. 11. Ion (above) and electron (below) density at t = 60 fs after the initial laser-droplet interaction, for a 1 μm radius droplet hit by a laser pulse of 40 fs duration and intensity I = 10^{20} W/cm^2. The density scale is logarithmic and goes up to 100 n_c.

This article is copyrighted as indicated in the article. Reuse of AIP content is subject to the terms at: http://scitation.aip.org/termsconditions. Downloaded to IP: 134.94.122.242 On: Tue, 18 Aug 2015 12:55:05

case, and on the other side the 16-cycle pulse is able to generate a shock shell propagating at the outer surface where the most energetic protons are sitting. The energies of the ions emitted by the 100 nm droplet by means of the shock generation mechanism are larger than those which could be obtained by the action of the ambipolar field mechanism only, as for the bigger droplets with $R \approx 0.5 - 1$ μm. However, the energy scaling exhibited by the two-cycle laser pulse as in Fig. 4 is steeper and more favorable in terms of the number of particles accelerated at the highest intensities ($>10^{21}$ W/cm^2) examined here. As there are currently a number of high-intensity few-cycle laser systems being developed, we hope that this study will motivate experimental interest in ion acceleration in this regime.

ACKNOWLEDGMENTS

The authors gratefully acknowledge the computing time granted by the VSR and JARA-HPC commissions through Project No. JZAM04 on the supercomputer JUQUEEN at Forschungszentrum Jülich.

[1]S. C. Wilks, A. B. Langdon, T. E. Cowan, M. Roth, M. Singh, S. Hatchett, M. H. Key, D. Pennington, A. MacKinnon, and R. A. Snavely, "Energetic proton generation in ultra-intense laser-solid interactions," Phys. Plasmas **8**, 542 (2001).
[2]R. A. Snavely, M. H. Key, S. P. Hatchett, T. E. Cowan, M. Roth, T. W. Phillips, M. A. Stoyer, E. A. Henry, T. C. Sangster, M. S. Singh, S. C. Wilks, A. MacKinnon, A. Offenberger, D. M. Pennington, K. Yasuike, A. B. Langdon, B. F. Lasinski, J. Johnson, M. D. Perry, and E. M. Campbell, "Intense high-energy proton beams from Petawatt-laser irradiation of solids," Phys. Rev. Lett. **85**, 2945 (2000).
[3]E. L. Clark, K. Krushelnick, J. R. Davies, M. Zepf, M. Tatarakis, F. N. Beg, A. Machacek, P. A. Norreys, M. I. K. Santala, I. Watts, and A. E. Dangor, "Measurement of energetic proton transport through magnetized plasma from intense laser interaction with solids," Phys. Rev. Lett. **84**, 670 (2000).
[4]Y. Fukuda, H. Sakaki, M. Kanasaki, A. Yogo, S. Jinno, M. Tampo *et al.*, "Generation of 50 MeV/u H ions in laser-driven ion acceleration with cluster-gas targets," SPIE Proc. **8779**, 87790F (2013).
[5]I. Pomerantz, J. Blakeney, G. Dyer, L. Fuller, E. Gaul, D. C. Gautier, D. Jung, A. R. Meadows, R. Shah, C. Wang, J. C. Fernandez, T. Ditmire, and B. M. Hegelich, "Laser-ion acceleration from transparent overdense plasmas at the Texas Petawatt," SPIE Proc. **8779**, 87791L (2013).
[6]A. Macchi, M. Borghesi, and M. Passoni, "Ion acceleration by superintense laser-plasma interaction," Rev. Mod. Phys. **85**, 751 (2013).
[7]A. Henig, D. Kiefer, M. Geissler, S. G. Rykovanov, R. Ramis, R. Horlein, J. Osterhoff, Zs. Major, L. Veisz, S. Karsch, F. Krausz, D. Habs, and J. Schreiber, "Laser-driven shock acceleration of ion beams from spherical mass-limited targets," Phys. Rev. Lett. **102**, 095002 (2009).
[8]A. P. L. Robinson, M. Zepf, S. Kar, R. G. Evans, and C. Bellei, "Radiation pressure acceleration of thin foils with circularly polarized laser pulses," New J. Phys. **10**, 013021 (2008).
[9]B. Qiao, S. Kar, M. Geissler, P. Gibbon, M. Zepf, and M. Borghesi, "Dominance of radiation pressure in ion acceleration with linearly polarized pulses at intensities of 10^{21} W/cm^2," Phys. Rev. Lett. **108**, 115002 (2012).
[10]B. Qiao, M. Zepf, M. Borghesi, B. Dromey, M. Geissler, A. Karmakar, and P. Gibbon, "Radiation pressure acceleration of ion beams from nano-foil targets: The leaky light-sail regime," Phys. Rev. Lett. **105**, 155002 (2010).
[11]T. Ditmire, J. Zweiback, V. P. Yanovski, T. E. Cowan, G. Hays, and K. B. Warton, "Nuclear fusion from explosions of femtosecond laser-heated clusters," Nature **398**, 489–492 (1999).
[12]J. Zweiback, R. A. Smith, T. E. Cowan, G. Hays, K. B. Wharton, V. P. Yanovsky, and T. Ditmire, "Nuclear fusion driven by Coulomb explosions of large deuterium clusters," Phys. Rev. Lett. **84**, 2634 (2000).
[13]J. Zweiback, T. E. Cowan, J. H. Hartley, R. Howell, K. B. Wharton, J. K. Crane, V. P. Yanovsky, and G. Hays, "Detailed study of nuclear fusion from femtosecond laser-driven explosions of deuterium clusters," Phys. Plasmas **9**, 3108 (2002).
[14]K. J. Mendham, J. W. G. Tisch, M. B. Mason, N. Hay, R. A. Smith, and J. P. Marangos, "Multi-keV proton energies form exploding hydrogen clusters," J. Phys. B.: At., Mol. Opt. Phys. **35**, 663 (2002).
[15]S. Sakabe, S. Shimizu, M. Hashida, F. Sato, T. Tsuyukushi, K. Nishihara, S. Okihara, T. Kagawa, Y. Izawa, K. Imasaki, and T. Iida, "Generation of high-energy protons from the Coulomb explosion of hydrogen clusters by intense femtosecond laser pulses," Phys. Rev. A **69**, 023203 (2004).
[16]J. Psikal, J. Limpouch, S. Kawata, and A. A. Andreev, "PIC simulations of femtosecond interactions with mass-limited targets," Czech. J. Phys. **56**, B515 (2006).
[17]J. Limpouch, J. Psikal, A. A. Andreev, K. Yu. Platonov, and S. Kawata, "Enhanced laser ion acceleration from mass-limited targets," Laser Part. Beams **26**, 225 (2008).
[18]S. Ter-Avetisyan, M. Schnurer, S. Busch, E. Risse, P. V. Nickles, and W. Sandner, "Spectral dips in ion emission emerging from ultrashort laser-driven plasmas," Phys. Rev. Lett. **93**, 155006 (2004).
[19]M. Schnurer, S. Ter-Avetisyan, S. Busch, E. Risse, M. P. Kalachnikov, W. Sandner, and P. V. Nickles, "Ion acceleration with ultrafast laser driven water droplets," Laser Part. Beams **23**, 337 (2005).
[20]See http://ccpforge.cse.rl.ac.uk/gf/project/epoch for extendable PIC open collaboration project UK.
[21]L. Di Lucchio and P. Gibbon, "Particle emission in laser-droplet interaction," in *Proceeding of the Europhysics Conference Abstracts 2014* (EPS, 2014).
[22]L. Di Lucchio and P. Gibbon, "Relativistic attosecond electron bunch emission from few-cycle irradiated nanoscale droplets," Phys. Rev. ST Accel. Beams **18**, 023402 (2015).
[23]T. V. Liseykina, S. Pirner, and D. Bauer, "Relativistic attosecond electron bunches from laser-illuminated droplets," Phys. Rev. Lett. **104**, 095002 (2010).
[24]F. V. Hartemann, S. N. Fochs, G. P. Le Sage, N. C. Luhmann, Jr., J. G. Woodworth, M. D. Perry, Y. J. Chen, and A. K. Kerman, Phys. Rev. E **51**, 4833 (1995).
[25]A. A. Andreev and K. Yu Platonov, "Self-similar regime without quasi-neutral approximation of ion acceleration in expanding plasma," Proc. SPIE **5482**, 93 (2004).
[26]M. Murakami and M. M. Basko, "Self-similar expansion of finite size non-quasi-neutral plasmas into vacuum," Phys. Plasmas **13**, 012105 (2006).
[27]C. Peltz, C. Varin, T. Brabec, and T. Fennel, "Fully microscopic analysis of laser-driven finite plasmas using the example of clusters," New J. Phys. **14**, 065011 (2012).
[28]L. O. Silva, M. Marti, J. R. Davies, R. A. Fonseca, C. Ren, F. S. Tsung, and W. B. Mori, "Proton shock acceleration in laser-plasma interactions," Phys. Rev. Lett. **92**, 015002 (2004).
[29]A. E. Kaplan, B. Y. Dubetsky, and P. L. Shkolnikov, "Shock shells in Coulomb explosion of nanoclusters," Phys. Rev. Lett. **91**, 143401 (2003).
[30]S. C. Wilks, W. L. Kruer, M. Tabak, and A. B. Langdon, "Absorption of ultra-intense laser pulses," Phys. Rev. Lett. **69**, 1383 (1992).

This article is copyrighted as indicated in the article. Reuse of AIP content is subject to the terms at: http://scitation.aip.org/termsconditions. Downloaded to IP: 134.94.122.242 On: Tue, 18 Aug 2015 12:55:05